J Anesth (1999) 13:197–204

Journal of
Anesthesia

Quantitative determination of arterial wall mechanics with pulse oximetric finger plethysmography

Rie Kato[1], Jiro Sato[1], Toshihiko Iuchi[2], and Yoshinori Higuchi[2]

Departments of Anesthesiology[1] and Neurosurgery[2], Chiba University School of Medicine, 1-8-1 Inohana, Chuo-ku, Chiba 260-8670, Japan

Abstract

Purpose. The plethysmographic wave of pulse oximetry reflects arterial pulsation at the fingertip. Since arterial pressure and the pulsatile component of the arterial cross section represent the input and output of the fingertip arterial system, respectively, arterial wall mechanics may be delineated from their relationship. We aimed to construct a mathematical model of the fingertip arterial wall from the relationship between the plethysmographic wave and arterial pressure.

Methods. The pulse oximetric plethysmograpic signal at the forefinger and pressure at the ipsilateral radial artery were measured. Employing the data, simple mathematical models with one to four mechanical elements were tested in terms of the goodness of fit and the physiological implications. The determined model was applied to the data obtained during administration of vasoactive agents in anesthetized patients.

Results. The mathematical model suited for describing arterial wall mechanics was a four-element, two-compartment model. The two compartments represent passive mechanical and active contractile properties, respectively. In the application of the model to the anesthetized patients, the vasoactive agents produced changes in the model parameters that implied mechanical alterations in the arterial wall.

Conclusion. These findings suggest the benefit of the four-element, two-compartment model in analyzing peripheral vascular wall mechanics influenced by various stimuli in intensive care and anesthesia.

Key words: Pulse oximetric plethysmography, Vascular wall mechanics, Mathematical model

Introduction

Pulse oximetry has been widely accepted as one of the most essential monitors of arterial oxygenation during the perianesthetic period. Its plethysmographic signal (ΔL) has been used as a qualitative indicator of the peripheral circulation [1–4]. In principle, ΔL is created by the pulsatile component of the blood flow of an artery across which light emitted from the oximeter passes [5]. Accordingly, the amplitude and shape of ΔL reflect the arterial caliber pulsation. If the artery is considered as a mechanical system, the arterial pulse pressure (ΔABP) and the pulsatile fraction of the arterial cross section are the input and output of the arterial system, respectively. From the relationship between ΔL and ΔABP, therefore, a mathematical model of wall mechanics of the fingertip artery could be derived [6]. The model would allow a quantitative description of the mechanical properties of peripheral arteries that are modulated by various circulatory stimuli during anesthesia.

The objectives of this study were to develop a simple mathematical model that describes the mechanical properties of the fingertip arterial wall, and to examine the validity of the model by applying it to the data obtained during administration of vasoactive agents in anesthetized patients.

Methods

After obtaining approval from our institutional ethics committee, we performed the study with informed consent of all subjects and patients.

Measurement of plethysmographic signal (ΔL)

We used a pulse oximeter system (M1020A, Hewlett-Packard, San Francisco, CA, USA) that possessed a linear relationship between ΔL and the pulsatile component of optical length. The light emitter and detector were separated from the pulse oximetry probe. They were affixed to the tip of the forefinger with a transpar-

Address correspondence to: J. Sato

Received for publication on March 10, 1999; accepted on June 24, 1999

ent two-sided adhesive tape so that the tissue between the emitter and the detector was not compressed. The oximeter automatically optimized the voltage gain of ΔL at the initial attachment of the probe and kept the gain constant thereafter. Since the level of voltage optimization varies among subjects, the measurement does not yield interindividual comparisons of ΔL, but it allows intraindividual observations of the temporal changes in ΔL.

Light projected from the emitter might cross more than one artery; henceforth, ΔL would represent the summed pulsation of the involved arteries. Provided that the arteries pulsate in synchrony with one another, we can assume that a single artery characterizes the summed mechanical behavior of those arteries.

Part I: Model development

We studied three healthy male volunteers (age 28, 28, and 38 years) recruited from our department. The subjects lay in the supine position in a room where the ambient temperature was kept constant at 25°C in order to maintain the subjects' peripheral circulation. The pulse oximetry probe was placed on the forefinger as described. Arterial pressure (ΔABP) was measured continuously through a catheter (24 gauge) placed in the ipsilateral radial artery (M1094A, Hewlett Packard). ΔL and ΔABP were sampled for 60 sec. and stored in a personal computer for off-line analysis.

A 20-heartbeat segment that showed stable signals was selected from each recording. Both ΔL and ABP signals were divided at end-diastolic points into consecutive single-beat signals. The 20 single-beat signals were averaged to obtain the representative single-beat signals that were used in the following model construction. The input and output of the fingertip artery as a mechanical system are ΔABP and the cross-sectional area (ΔArea), respectively. Since the pulsatile fraction of the arterial caliber is proportional to log(ΔL) [5], we calculated ΔArea from ΔL of the averaged signals as

$$\Delta\text{Area} = 2\pi\left(\log\left(\Delta L\right)\right)^2 \Big/ \left|\text{Max} - \text{Min}\right|$$

where Max and Min denote the maximum and minimum of $2\pi(\log(\Delta L))^2$, respectively. The range of ΔArea was normalized to be one, since the voltage gain of ΔL was determined arbitrarily by the oximeter and differed among subjects. Plots of ΔABP versus ΔArea in a representative subject are presented in Fig. 1.

Model fitting. We examined only linear models, since ΔL signal did not produce sufficient resolution to yield sophisticated modeling with nonlinear mechanical elements. The models were fitted to the data by multiple linear regression. Improvements of model fittings were tested by the partial *F* test [7]. When a model presented significant improvement over the other model with $P < 0.05$ in all three subjects, it was considered to be significantly better.

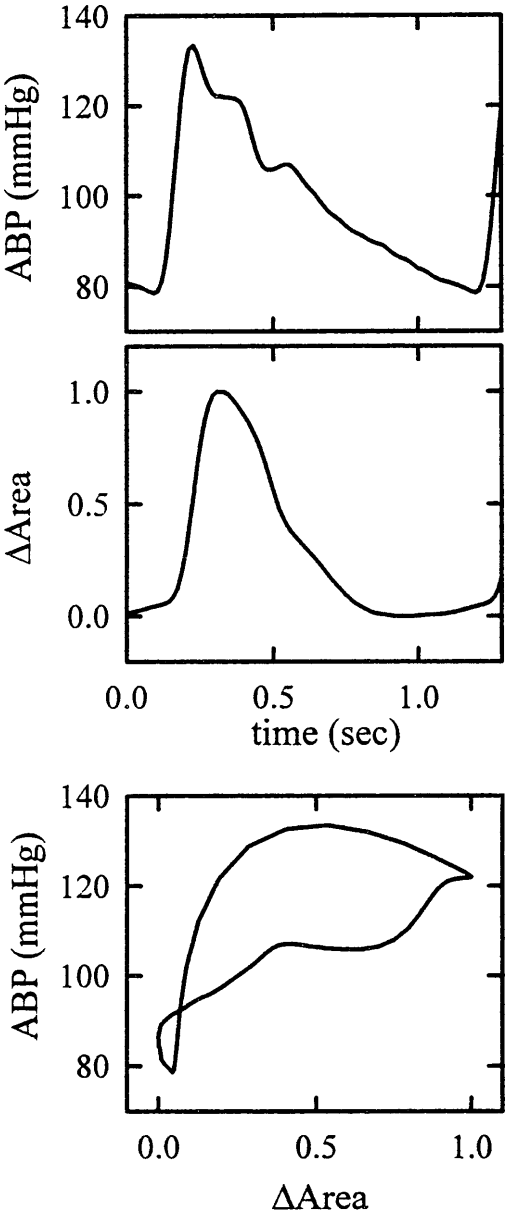

Fig. 1. Example of averaged single-heartbeat signals in a representative subject. *Upper two panels* show ABP and ΔArea. *Bottom panel* shows ABP–ΔArea plot

The first model examined consisted of only one mechanical element, a spring, whose mechanics were described by elastance E (Fig. 2A). The equation of motion of the model is

$$\Delta\text{ABP} = \text{E}\,\Delta\text{Area}.$$

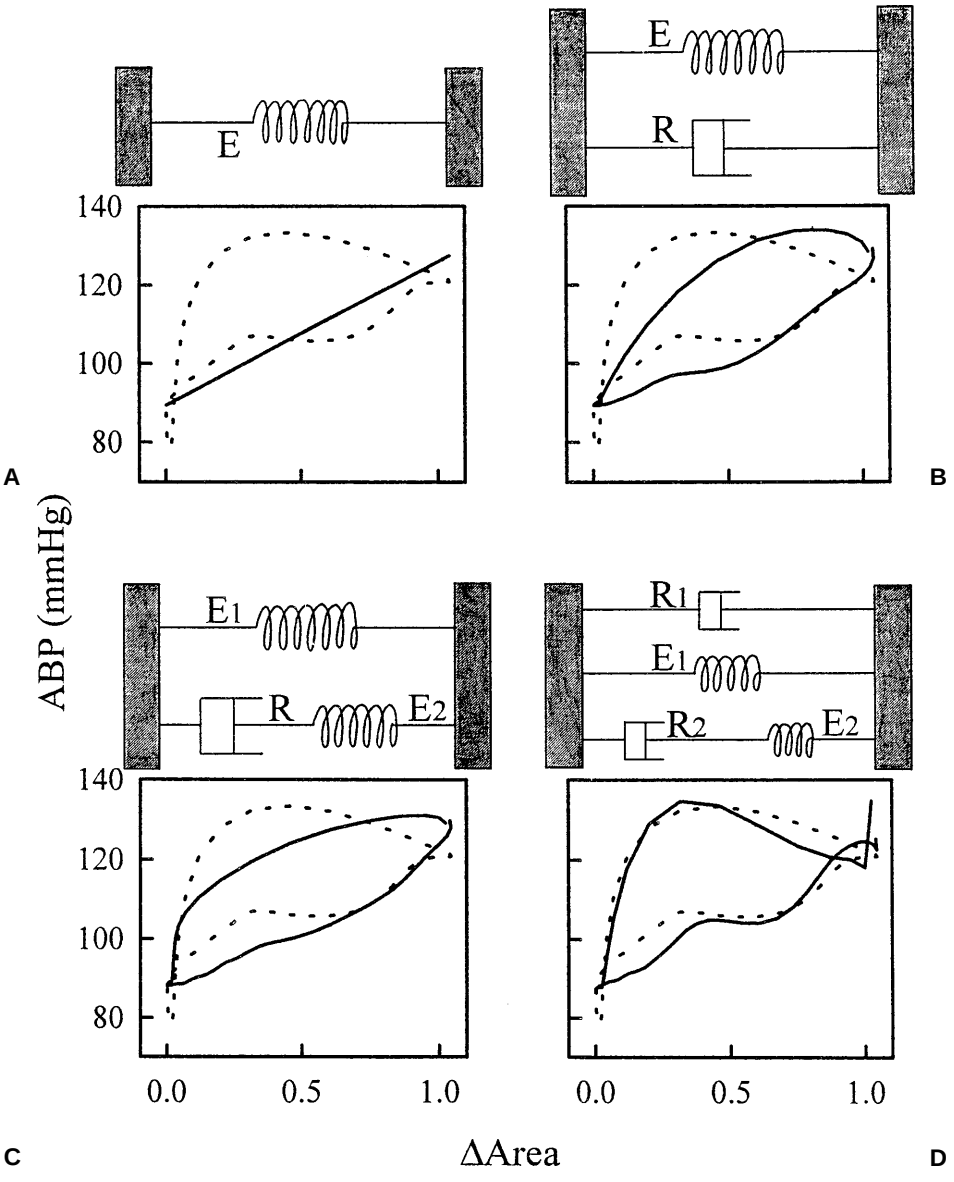

Fig. 2. Mathematical models considered for the model development. *E* and *R* denote elastance (spring) and resistance (dashpot), respectively. **A** Simplest model with a spring. **B** Parallel dashpot (*R*)-spring (*E*) model (Voigt body). **C** Three-element model (Kelvin body). **D** Four-element viscoelastic model. *Solid* and *dotted lines* indicate the data and the best-fit model in a representative subject, respectively

Since in this model there is only a linear relationship between ΔArea and ΔABP, it is unable to explain the hysteresis loop observed in the data. In the second model, we added a dashpot element (resistance R) in parallel to the spring (Fig. 2B):

$$\Delta\mathrm{ABP} = \mathrm{R}\,d(\Delta\mathrm{Area})/dt + \mathrm{E}\,\Delta\mathrm{Area}.$$

This two-element model, called the Voigt body, is used to describe the viscoelastic properties of biological tissues such as lung parenchyma, artery, and relaxed skeletal and smooth muscles [8–11]. Although the model could explain part of the looping, a substantial discrepancy between the data and the model remained. The third model consisted of a spring and a spring-dashpot element (Maxwell body) (Fig. 2C):

$$\mathrm{R}\,d(\Delta\mathrm{ABP})/dt + \mathrm{E}_1\,\Delta\mathrm{ABP} = \mathrm{R}(\mathrm{E}_1 + \mathrm{E}_2)d(\Delta\mathrm{Area})/dt + \mathrm{E}_1\mathrm{E}_2\,\Delta\mathrm{Area}.$$

This model, called the Kelvin body, has also been used to describe biological tissue rheology [8–11]. The improvement of fit over the second model was statistically insignificant, despite the increased number of parameters. The final model considered included four mechanical elements. A resistance was added in parallel to the third model [12] (Fig. 2D):

$$d(\Delta\mathrm{ABP})/dt + \Delta\mathrm{ABP} = \mathrm{R}_1\mathrm{R}_2\,d^2(\Delta\mathrm{area})/dt^2 + \left[(\mathrm{E}_1 + \mathrm{E}_2)/\mathrm{R}_1 + \mathrm{E}_2/\mathrm{R}_2\right]d(\Delta\mathrm{Area})/dt + \mathrm{E}_1\mathrm{E}_2\Delta\mathrm{Area}.$$

Table 1. Parameter values of the four-element model[a]

Subject	R_1	E_1	R_2	E_2
1	1.00	13.84	−1.45	−11.08
2	1.00	15.84	−1.89	−8.41
3	1.00	13.94	−1.78	−12.27

[a] Values of the parameters E_1, R_2, and E_2 are expressed as ratios to R_1.

This model significantly improved fitting ($P < 0.01$ for all subjects). The parameter values, shown in Table 1, are expressed as the ratios to R_1, since their absolute values do not have any physiological meaning. The values of R_1 and E_1 were positive, whereas those of R_2 and E_2 were negative in all subjects.

The physiological implications of these parameter values should be considered. For example, extraneous energy is required for a spring to be compressed from its resting length. This energy is stored in the spring while it is compressed and released when it recovers its resting length. This is termed passive behavior with a positive value of elastance. Negative elastance implies a stress–strain relationship that has a direction opposite to this. That is, a spring with negative elastance compresses itself while releasing energy. For a system composed of only passive mechanical elements, it is physically impossible to bear negative elastance and resistance. Contraction of vascular smooth muscle might be a mechanical candidate for negative R_2 and E_2. As the smooth muscle contracts, it produces heat as a result of active work, exhibiting energy flux with the direction opposite to that of passive components [11,13–15]. The force–length relationship of smooth muscle during contraction resembles the mirror image of that of a passive elastance–resistance system [13–15]. We, therefore, allotted the negatively parameterized mechanical elements to the active mechanical force generated by vascular smooth muscle.

Part II: Application of the model to the data obtained during anesthesia

The aim of Part II of the study was to examine the physiological implications of the model by applying it to the clinical data. Forty-two patients (age 27–74 years) with no respiratory or circulatory complications participated in this study. Anesthesia was maintained with oxygen–nitrous oxide–isoflurane, with or without epidural lidocaine. We selected 11 subjects whom we treated with vasoactive agents for circulatory variations. ΔL and ABP signals were monitored as in Part I of the study. When patients presented with hypotension (five patients) or hypertension (six patients), we administered intravenous phenylephrine or nicardipine, respectively, at appropriate bolus doses (0.1–0.2 mg of phenylephrine, 1–2 mg of nicardipine). Data sampling was commenced 1 min before administration and continued until ABP returned to the preadministration values. The vasoactive drugs usually produced transient changes of 30–40 mmHg in ABP. The duration of data sampling ranged from 7 to 10 min. The data were stored in a computer for off-line analysis. No patient had severe circulatory complications during anesthesia.

The data were segmented into consecutive single-beat signals as described in Part I. In this study, ΔArea of each single beat was scaled for normalization by dividing by the average ΔArea of the preadministration phase, since ΔArea was in arbitrary units that differed among subjects. The four-parameter model constructed in Part I was applied to each single-beat signal consecutively. The parameter values were expressed as the ratios to R_1 at the preadministration phase. This allowed the beat-wise temporal observation of relative changes in the parameters.

Results

Figure 3 shows examples of changes in heart rate, ΔArea, and ABP after the administration of phenylephrine or nicardipine in representative patients. Phenylephrine produced a marked transient decrease in ΔArea, which did not necessarily indicate a decrease in the arterial cross section (i.e., vascular constriction), but reflected a decrease in its pulsatile component. Compared with phenylephrine, nicardipine had a small effect on ΔArea, indicating a small change in arterial pulsation; however, this does not necessarily suggest that significant arterial dilation was not produced.

Figure 4 presents temporal changes in the model parameters after the administration of phenylephrine in individual subjects. R_1 showed a rapid increase followed by a gradual decrease toward the preadministration value, whereas R_2, in general, exhibited a decrease followed by a gradual recovery. In contrast, both E_1 and E_2 showed rather complicated behavior. The changes often seemed discontinuous and showed rapid transient jumps. The changes were associated with changes of sign in some cases (cases 1, 2, 4 and 5). The discontinuous changes were usually replaced by smooth recovery trends.

Figure 5 shows changes in the parameters created by a bolus infusion of nicardipine. Compared with phenylephrine, nicardipine produced smaller and smoother trends. In general, nicardipine produced decreases in the magnitudes of all parameters except R_2. R_2 did not show changes reproducible in all patients.

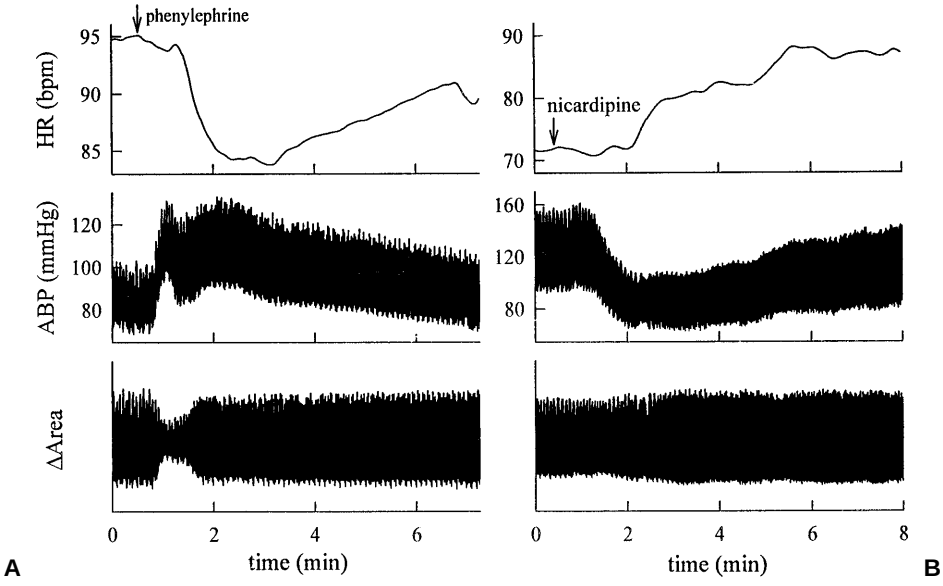

Fig. 3. Examples of changes in heart rate (*HR*), ABP, and ΔArea after the administration of (**A**) phenylephrine and (**B**) nicardipine in representative patients

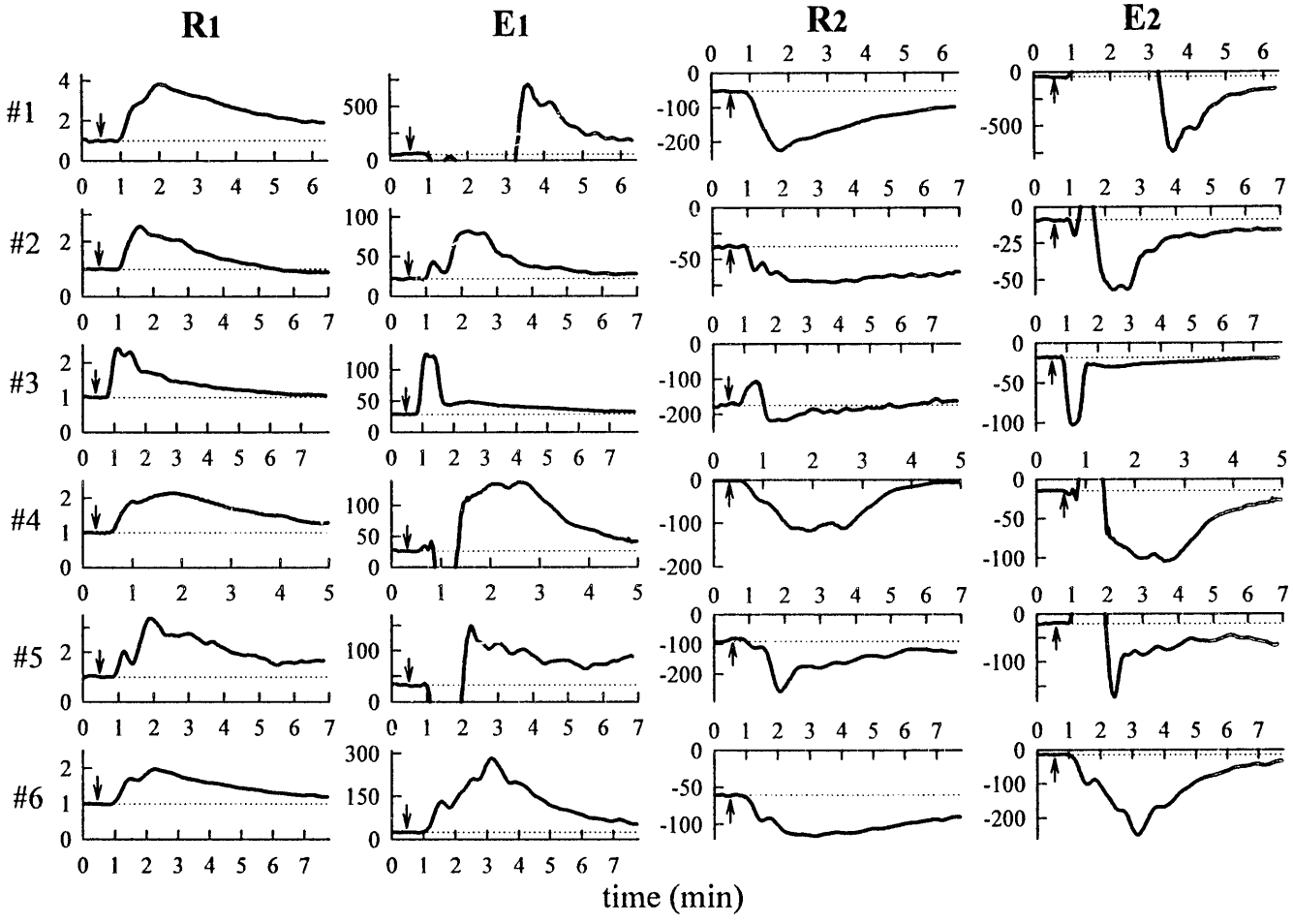

Fig. 4. Changes in model parameters after the administration of phenylephrine in individual subjects. *Dotted lines* indicate preadministration values. Each parameter is plotted on either the plus or the minus side of the Y-axis according to the physiological interpretation of the model. After administration, some patients showed transient discontinuity, such as sudden jumps with or without changes in sign of E_1 and E_2

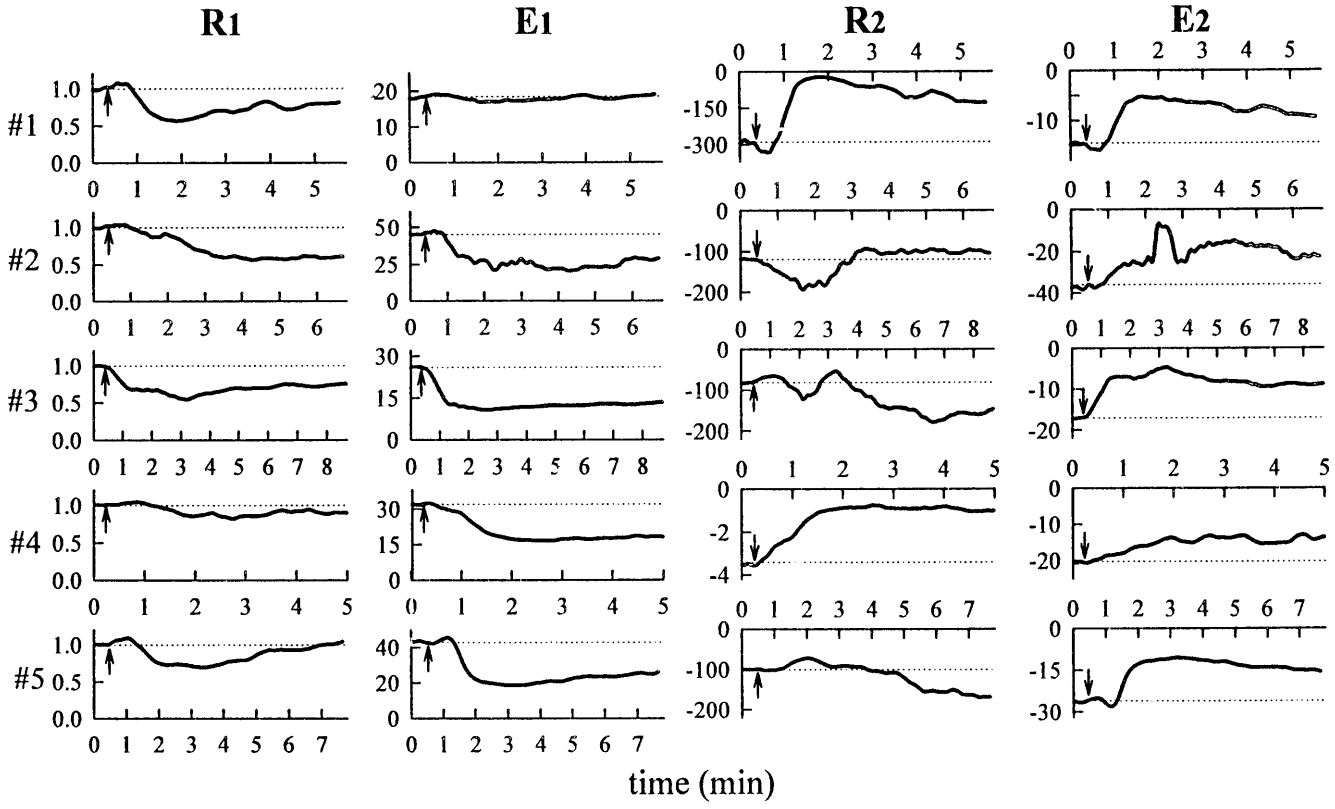

Fig. 5. Changes in model parameters after the administration of nicardipine in individual subjects. *Dotted lines* indicate preadministration values

Discussion

This study differs from previous studies on vascular wall mechanics [9–11,16–19] in the following ways. The previous studies performed direct measurements of the diameter or cross-sectional area of a single artery while applying static or quasi-static pressure perturbations directly to the artery. This allowed precise identification of mechanical structure and refined model construction. On the other hand, the present study measured a relative and summed quantity of the pulsatile cross sections of the whole fingertip vasculature. Furthermore, we did not directly measure the pressure of the fingertip artery itself, but substituted the radial arterial pressure for it. Although these indirect approaches might produce some estimation errors in the model parameters, we believe that the error was practically negligible, since the constructed model was still simple enough. In addition, the arteries we measured were much smaller than those studied previously (brachial artery, carotid artery, or aorta). Fingertip arteries would produce much greater dilation or constriction responses to vasoactive stimuli than the larger arteries during anesthesia [14,20]. Since physiological interpretation of modeling results would depend on the experimental design [13,15] (vascular size, static or dynamic measurement, model structure, etc.), we cannot compare our results simply with the previous studies. However, the ratio of elastance to resistance obtained in the present study is comparable to the result of Armentano et al. [17].

One of the key points in the developed model is that the active contraction of vascular smooth muscle was allocated to the negatively parameterized mechanical elements. The physiological interpretation for this was incorporated into the modeling process as follows. Unifying the previously proposed models [9–12,15,17], we constructed a mechanical model of the arterial wall with physiological homology (Fig. 6A). The model consists of a connective tissue component connected in parallel with a smooth muscle component. The connective tissue component is composed of only passive elements. It represents connective tissues, such as adventitia and media, constituted mainly by elastic and collagen fibers. On the other hand, the smooth muscle component, representing the mechanical properties of vascular smooth muscle, consists of active contractile and passive mechanical elements. We rearranged and simplified this model to correlate with our model, fitting the results of Part I (Fig. 6B). The simplified version is

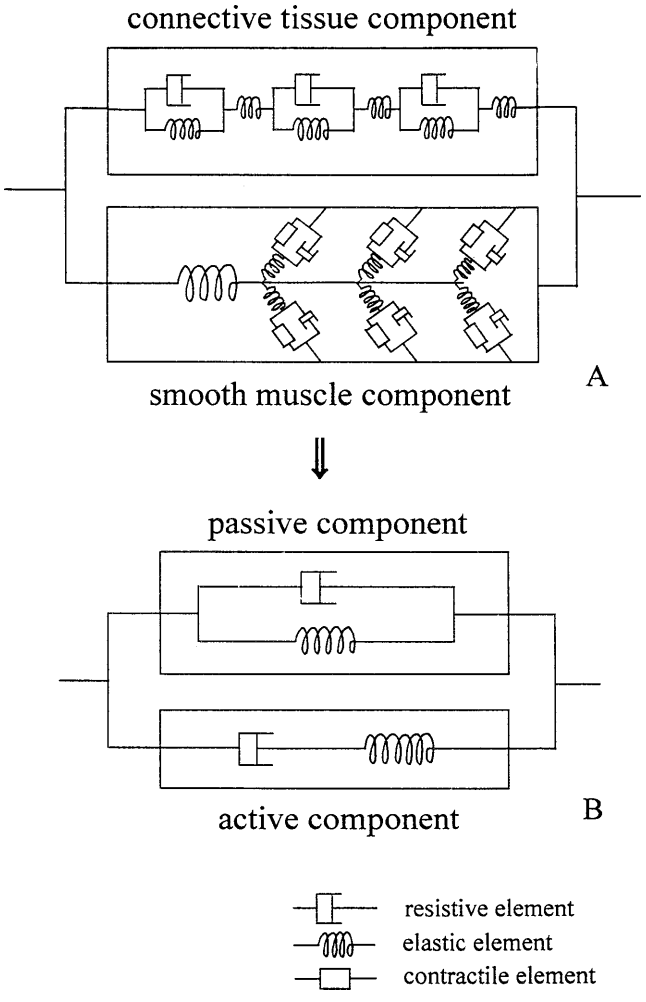

Fig. 6. Mechanical model of arterial wall. **A** Arterial wall consists of a connective tissue and a smooth muscle component. **B** Rearranged and simplified model. The model is identical to the four-parameter model created by model development in Part I of the study (Fig. 2D)

partitioned into two components, each of which is composed of only passive or only active elements. The passive component represents the summed behavior of both the connective tissue component and the passive elements of the smooth muscle component in the model of Fig. 6A. It corresponds to the unit described by positive parameters R_1 and E_1 of our four-parameter model shown in Fig. 2D. In contrast, the active component represents only active dynamics generated by contractile elements of the smooth muscle component. Its mechanical behavior is expressed by negative parameters R_2 and E_2.

In a physiological sense, the parameters (E_2 and R_2) for active contraction of the vascular smooth muscle represent the stiffness (resting tone) and the velocity of contraction of the smooth muscle, respectively. Generally speaking, phenylephrine increased the magnitudes of all parameters, whereas nicardipine decreased those of all but R_2. Increases in E_2 and R_2 observed after phenylephrine may reflect both the increased resting tone and the contraction velocity of vascular smooth muscle. That nicardipine reduced E_2 but not R_2 might indicate that nicardipine reduced the resting tone (softened the smooth muscle) but did not affect the contraction velocity.

The passive mechanical parameters E_1 and R_1 also changed in response to the administration of vasoactive agents, indicating that these agents alter the properties of mechanically passive tissues, mainly elastic and collagen fibers. It is suggested that passive mechanical properties (elasticity and viscosity) are manifested not only by specific tissues such as elastin, collagen, and relaxed smooth muscle, but also by the mechanical coupling as a result of the network structure of these tissues [17,19,20]. Part of the passive mechanical properties is manifested even by the force generation of smooth muscle and the myogenic response to stretching [10,11,15,17,18]. The concomitant changes in the passive (R_1 and E_1) and active (R_2 and E_2) parameters observed in our model may be produced by this mechanical coupling of passive and active components.

The transient discontinuity in E_1 and E_2 observed immediately after the administration of phenylephrine indicates that the present model is unable to describe the acute phase of mechanical changes produced by phenylephrine. Arterial wall elasticity is known to be nonlinear and dependent on pressure (force) and diameter (length) [21]. Arterial smooth muscle also has highly nonlinear mechanics dependent on the level of muscle activation generated by vasoconstrictors [16,18]. This nonlinearity may be a reason for the discontinuity in the model parameters.

Indeed, our model has limitations in describing the mechanics of the peripheral vascular wall. Our analysis cannot be performed on patients with insufficient peripheral circulation, whichs produce poor plethysmographic signals. This is also the case when the peripheral vascular wall exhibits complex mechanical changes, as was produced by phenylephrine in our study. However, provided that signal reliability is assured, the four-element, two-compartment model would be useful for analyzing peripheral vascular mechanics, which are vulnerable to changes due to various factors during anesthesia and intensive care, such as bleeding, vasoactive agents, and the thermal environment.

References

1. Kim J-M, Arakawa K, VonLintel T (1975) Use of the pulse-wave monitor as a measurement of diagnostic sympathetic block and of surgical sympathetectomy. Anesth Analg 54:289–296

2. Kim J-M, LaSalle AD, Parmley RT (1977) Sympathetic recovery following lumbar epidural and spinal analgesia. Anesth Analg 56:352–355
3. Partridge BL (1987) Use of pulse oxymetry as a noninvasive indicator of intravascular volume status. J Clin Monit 3:263–268
4. Vegfors M, Tryggvason B, Sjberg F, Lennmarken C (1990) Assessment of peripheral blood flow using a pulse oximeter. J Clin Monit 6:1–4
5. Yoshiya I, Shimada Y, Tanaka K (1980) Spectrophotometric monitoring of arterial oxygen saturation in the fingertip. Med Biol Eng Comput 18:27–32
6. Shearer JL, Murphy AT, Richardson HH (1967) Modeling of physical systems. In: Introduction to system dynamics. Addison-Wesley, Reading, Massachusetts, pp 150–160
7. Kleinbaum DG, Kupper LL, Muller KE (1988) Testing hypotheses in multiple regression. In: Applied regression analysis and other multivariate methods, 2nd edn. PWS-Kent, Boston, pp 124–143
8. Fung YC (1993) The meaning of the constitutive equation. In: Biomechanics. Mechanical properties of living tissues, 2nd edn. Springer-Verlag, New York, pp 23–65
9. Dobrin P, Canfield T (1977) Identification of smooth muscle series elastic component in intact carotid artery. Am J Physiol 232:H122–H130
10. Cox RH (1978) Regional variation of series elasticity in canine arterial smooth muscles. Am J Physiol 234:H542–H551
11. Barra JG, Armentano RL, Levenson J, Fischer EIC, Pichel RH, Simon A (1993) Assessment of smooth muscle contribution to descending thoracic aortic elastic mechanics in conscious dogs. Circ Res 73:1040–1050
12. Bates JHT, Baconnier P, Milic-Emili J (1988) A theoretical analysis of interrupter technique for measuring respiratory mechanics. J Appl Physiol 64:2204–2214
13. Murphy RA (1980) Mechanics of vascular smooth muscle. In: Bohr DF, Somlyo AP, Sparks HV Jr (eds) Handbook of physiology. The cardiovascular system. Vol. II. Vascular smooth muscle. American Physiology Society, Bethesda, MD, USA, pp 325–351
14. Gow BS (1980) Circulatory correlates: vascular impedance, resistance, and capacity. In: Bohr DF, Somlyo AP, Sparks HV Jr (eds) Handbook of physiology. The cardiovascular system. Vol. II. Vascular smooth muscle. American Physiology Society, Bethesda, MD, USA, pp 353–408
15. Johnson PC (1980) The myogenic response. In: Bohr DF, Somlyo AP, Sparks HV Jr (eds) Handbook of physiology. The cardiovascular system. Vol. II. Vascular smooth muscle. American Physiology Society, Bethesda, MD, USA, pp 409–442
16. Jackson PA, Duling BR (1989) Myogenic response and wall mechanics of arterioles. Am J Physiol 257:H1147–1155
17. Armentano RL, Barra JG, Levenson J, Simon A, Pichel RH (1995) Arterial wall mechanics in conscious dogs. Assessment of viscous, inertial, and elastic moduli to characterize aortic wall behavior. Circ Res 76:468–478
18. Cox RH (1976) Effects of norepinephrine on mechanics of arteries in vitro. Am J Physiol 231:420–425
19. Bank AJ, Wilson RF, Kubo SH, Holte JE, Dresing TJ, Wang H (1995) Direct effects of smooth muscle relaxation and contraction on in vivo human brachial artery elastic properties. Circ Res 77:1008–1016
20. Rhodin JAG (1980) Architecture of the vessel wall. In: Bohr DF, Somlyo AP, Sparks HV Jr (eds) Handbook of physiology. The cardiovascular system. Vol. II. Vascular smooth muscle. American Physiology Society, Bethesda, MD, USA, pp 1–19
21. Fung YC (1993) Bioviscoelastic solids. In: Biomechanics. Mechanical properties of living tissues, 2nd edn. Springer-Verlag, New York, pp 242–320